In Situ Coherent Lidar (ISICL): sensitivity, sampling rate, and practical considerations for using a particle mapper in plasma chambers and other inhospitable places

Philip C. D. Hobbs and Marc A. Taubenblatt,

IBM Thomas J. Watson Research Center,
PO Box 218,
Yorktown Heights, NY 10598

ABSTRACT

The ISICL (*In Situ* Coherent Lidar) sensor is a recently described measurement device for sensing and mapping the temporal and spatial distribution of isolated submicron particles in semiconductor processing plasma chambers, fluid tanks, and other inaccessible or hostile places. It requires no modifications to the chamber, and senses the volume directly over the wafer, while the process is running. Its detection sensitivity is extremely high: even in a very bright plasma, it requires only 50 scattered photons to detect a particle at a false alarm rate of 10^{-5} Hz.

Here we present theoretical and experimental results for the sensitivity and volumetric sampling rate of the sensor, as well as a method of using the measured pulse height histogram to obtain particle size information, and some practical tests of performance vs. window quality and back wall material.

Keywords: in situ measurement, particle detectors, microcontamination, reactive ion etch, coherent lidar, ultrasensitive detection.

1. INTRODUCTION

Semiconductor manufacturers all over the world face steadily tightening requirements for cleanliness in processing equipment. As chip sizes grow, features shrink, the number of processing steps increases, and price pressure from other manufacturers intensifies, the number of particles per wafer per step must decrease rapidly. Processing tools for reactive-ion etch (RIE), chemical vapour deposition (CVD), and sputtering, to name only a few, have very short mean times between failure (MTBFs), only 100 to 300 hours in most instances.

The usual failure mode is out-of-control particle counts. These are measured by a monitor wafer run through the chamber once per day, or at most once per shift (coupled with occasional measurements of defects on patterned wafers). This approach has the advantage of familiarity and simplicity; one uses the count of added particles on a monitor wafer to predict the counts on product wafers, and the tools are already set up to run wafers, so no special handling or modifications are needed. Particle counters designed to work on bare wafers are faster, more sensitive, and less expensive than those which work on patterned wafers, so particles on monitors can be detected very sensitively.

The monitor technique suffers, unfortunately, from a number of serious limitations. The first is that a monitor wafer cannot usually be subjected to the real process, since most processes are sensitive to loading by the wafer surface, and a bare silicon or blanket film wafer presents a different surface composition than a real product wafer (real product wafers are not normally used for this purpose, as they are valuable, and particles are difficult to detect on patterned surfaces, especially as they may become embedded in the film being deposited).

The desire for a faster, more direct measurement of the contamination encountered by product wafers has motivated the development of the *In-Situ* Coherent Lidar (ISICL) sensor, which has been described in a previous paper[1]. That paper treated the sensor design and briefly reported the performance of a prototype system. Mitchell and Knollenberg have recently published a comparison of different *in situ* particle detectors for semiconductor processing tools[2], including pump line monitors and ISICL.

In this paper, we present experimental results for the sensitivity and sample volume of a newer version of the sensor in a simulated tool environment, and simple tests demonstrating that it can work with a difficult chamber wall finish and a poor quality window, both of which are important preconditions for real technological use. We constructed a testing apparatus consisting of a small chamber, which can be purged with filtered dry nitrogen, a commercial aspirator system for introducing monodisperse spheres of polystyrene latex (PSL) from suspension, and a laser aerosol particle counter (LPC) for comparison. Spheres of different diameters were introduced into the chamber, and the concentration measured using the LPC; the volume sampling rate of the ISICL sensor was obtained by dividing the count rate obtained by the known particle concentration.

The sensor reports x and y position of the particles, together with the peak height of the received signal. Because the trajectory of the particle through the beam is unknown, there is no unique mapping from a pulse height to a particle size (or even to a definite scattering cross section); nevertheless, because the sensitivity falls off faster than exponentially with cross axis distance, even the smeared data allows binning particles to within a factor of 2 in diameter. It is possible in principle to statistically transform a pulse height histogram to a scattering cross section histogram, but this will probably be unnecessary in technological applications, since the required size discrimination is usually coarse.

2. THE ISICL SENSOR

Since a detailed presentation of the design and operating principles of ISICL has been published, we will recap the system characteristics only briefly. ISICL is a coherent-detection laser radar (lidar) system for detecting particles in inaccessible or hostile volumes such as ovens, tanks, and plasma chambers.

As shown in Figure 1, It uses a rapidly scanned single-frequency laser beam, which enters the volume through a window of indifferent optical quality (see below). Light scattered from a particle near the focus of the beam comes back through the same window, and some of it is recollimated and caused to interfere with a local oscillator (LO) beam derived from the same laser. The received signal is a tone burst, whose amplitude records the strength of the scattered light pulse, and whose carrier frequency is set by the Doppler shift. The tone burst is filtered, amplified, and compared to a tracking threshold. Bursts which cross the threshold are accepted as particle events. Using backscatter simplifies scanning, since the received light is descanned by the same galvo mirrors used for the transmit beam. Backscatter operation also greatly reduces the optical access required; a single dirty window is sufficient. The main difficulties encountered when working in backscatter are somewhat smaller signals, due to the dependence of differential scattering cross section on the scattering angle, and, especially, the enormous background signal caused by the transmit beam reflecting from the back wall of the chamber,

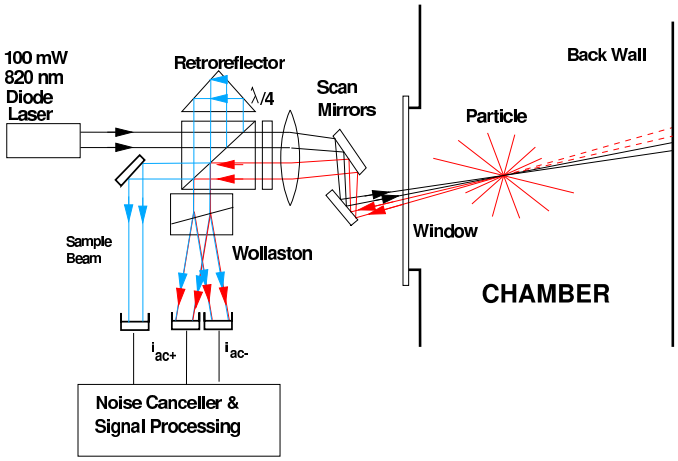

Figure 1: Optical schematic of the ISICL sensor (from Ref. 1).

which may be >10^6 times as strong as a nominally detectable particle signal. There are also a number of finer points, for which the earlier paper should be consulted.

3. THEORY

3.1. Coherent Detection

The scanned laser beam must be powerful (100-150 mW), because otherwise there are too few scattered photons available for very small particles to be detectable. Because the sensor must operate in an existing chamber, it is not in general possible to control what happens to this light after it passes through the focal region; in particular, we cannot usually put efficient beam dumps inside the chamber. Thus we must contend with light scattered from the chamber back wall. This light is approximately 10^6 times stronger than that from a nominally detectable particle, in the detected solid angle and bandwidth.

It is clearly impossible to use ordinary photon-counting to find a 50-photon signal in a fluctuating background this large. Baffles help considerably, but not enough to overcome such a factor. The only suitable candidate is coherent detection. Since this technique is still not widely used in technological applications, it is worthwhile presenting a short summary of the principle. A full presentation of this technique as applied to laser radar is available in a book by Jelalian[3]. A coherent detection system adds the scattered light field to a local-oscillator (LO) beam, and causes them to interfere on a photodiode. If the scattered field is Ψ_{scat}, and the local oscillator field is Ψ_{LO}, then the total photocurrent i_p from the photodiode is given by

$$i_p = K\int\int_{det} d^2x |\Psi_{scat} + \Psi_{LO}|^2 = K(i_{LO} + i_{scat} + i_{ac}), \quad (1)$$

where K is a constant, i_{LO}, i_{scat}, and i_{ac} are the photocurrents due to the LO beam alone, the scattered beam alone, and the interference of the two; they are given by

$$i_{LO} = K\int\int_{det} d^2x \, \Psi_{LO}\Psi_{LO}^* \quad (2)$$

$$i_{scat} = K\int\int_{det} d^2x \, \Psi_{scat}\Psi_{scat}^* \quad (3)$$

and

$$i_{ac} = 2K\,Re\left\{\int\int_{det} d^2x \Psi_{LO}\Psi_{scat}^*\right\} \quad (4)$$

If the two signals are mutually spatially coherent, their phases will have exactly the same spatial dependence, differing at most by an overall phase factor, which may depend on time; thus (4) becomes

$$i_{ac} = 2K\,Re\left\{\exp(i\phi(t))\int\int_{det} d^2x |\Psi_{scat}||\Psi_{LO}|\right\} \quad (5)$$

which providing the shapes of their amplitude distributions are the same as well, is

$$i_{ac} = 2\,i_{scat}\sqrt{\frac{i_{LO}}{i_{scat}}}\cos\phi(t) \quad (6)$$

The i_{ac} term is larger than the i_{scat} term by a factor of $(i_{LO}/i_{scat})^{1/2}$, Since i_{LO} is typically about 300 μA (from a local oscillator beam power of 0.5 mW), whereas i_{scat} may be only a few electrons in the measurement

time, this term represents a large gain if Ψ_{scat} is weak. In a bandwidth B, the shot noise of the LO beam contributes an rms noise current i_n given by

$$i_n = \sqrt{2 q i_{LO} B} \tag{7}$$

where q is the electron charge. To compute how large a value of i_{scat} is needed for i_{ac} to exceed the shot noise of the LO photocurrent, we equate the RMS values of i_n and i_{ac}, then solve to obtain for the noise-equivalent i_{scat},

$$\langle i_{scat} \rangle_{min} = qB \tag{8}$$

Note that if the peak value of the photocurrent is considered instead of the rms (as in a thresholding operation), the noise equivalent i_{scat} is reduced by a factor of $\sqrt{2}$. For the system at hand, the nominal detectable particle produces about 50 electrons in 3 microseconds, equivalent to a photocurrent of 2.7 pA; the gain due to coherent detection at that level is

$$A = \sqrt{\frac{2 i_{LO}}{i_{nom}}} \tag{9}$$

which is about 15,000.

The conclusion is that a scattered field, so weak that by itself it yields a detected photocurrent of only one electron per second in a one hertz bandwidth, can in a coherent detection system give rise to an ac photocurrent whose rms value is equal to the rms shot noise i_n of the local oscillator, independent of the value of i_{LO}. For a slightly stronger signal, i_{ac} is proportional to $\sqrt{i_{scat}}$, and the noise is constant (since the total photocurrent is approximately i_{LO}), so the current signal to noise ratio (SNR) is equal to the square root of the number of scattered photons collected, just as in a dark-field photon counting system. Thus the SNR of the system is the SNR of the scattered field alone, not that of the local oscillator. While a coherent detection system can achieve the same accuracy in estimating the true amplitude of a small signal as a photon counter can, it is not as good at distinguishing the presence or absence of such a signal. An ideal photon-counting detector could in principle (on the assumptions of zero stray light and zero dark current) detect a particle with a single photon, whereas a coherent detector requires more photons in order to reduce its false alarm rate (see below). Despite this theoretical disadvantage, the strong stray light mandates the use of a coherent detector for this application.

Gain by itself does not improve the stray light rejection of the particle counter; fortunately, however, the coherent detector exhibits gain only for those scattered fields which are spatially and temporally coherent with the local oscillator beam. This provides a powerful means for discriminating against the stray light.

Provided that the detector is larger than the beam, and that no vignetting occurs elsewhere, the integrals in Eqs.1-5 can be evaluated at any plane in the optical system. In particular, they can be evaluated at an image of the sensitive volume itself. At an image plane, the LO beam Ψ_{LO} is large inside the focal region, and nearly zero elsewhere. Thus scattered light which fails to pass through the focal region will be multiplied by zero, and therefore fail to contribute to the ac photocurrent.

If the light comes from a point on the optical axis, but far out of focus, then by the time it gets to the focal plane, it will have spread out over a large area, and only a small portion of it will pass through the focal spot. Moreover, light passing through the focus, but not travelling along the axis of the LO beam, will have a phase which varies linearly across the focal spot of the LO beam, causing the product term to exhibit interference fringes which make the integral go to zero as the angular error becomes large.

Both of these effects are helpful in overcoming the huge stray light level. The falloff in the signal due to defocus is only polynomial with distance, since the fraction of the defocused light which nonetheless passes

through the focal spot goes as r^{-2} , whereas (for Gaussian beams), the falloff due to missing the focus or to being off-axis is exponential.
Returning to the system at hand, the effect of coherent detection is to reduce the ratio of the photocurrent i_{stray} (due to the stray light) to i_{ac} from 10^6 to approximately 100. Together with a simple baffle arrangement, this is sufficient to solve the stray light problem, although problems may still be encountered if there is strong stray light coming directly along the axis of the LO beam.

Together with the laser noise canceller[4], which reduces the effects of amplitude noise on the LO beam, plus automatic adjustment of the diode laser injection current to reduce mode hopping noise, this improvement is sufficient to allow measurement performance limited by the photon statistics of the scattered light ψ_{scat}.

3.2. Sample Volume/Sensitivity Tradeoff

The sensitivity of the particle counter is given by the minimum number of photons it requires in order to detect a particle. For a particle in the centre of the sensitive region, the scattered intensity is the product of the transmit beam intensity times the differential scattering cross section of the particle, times the detector solid angle. Since we know that the shot noise level is equivalent to one coherently detected "noise" photon in 1 Hz, it is convenient to work in units of photons, since that yields the signal to noise ratio directly.

For a Gaussian transmit beam of power P at wavelength λ, focused at a numerical aperture NA, the photon flux at the beam waist is

$$F(\boldsymbol{P},\lambda,\boldsymbol{NA}) = \frac{2\pi \boldsymbol{NA}^2 \boldsymbol{P}}{\lambda hc} \tag{10}$$

From Eq. 4, assuming that the intensity of the scattered light is constant over the detector aperture, the effective detector solid angle is

$$\Omega_{\boldsymbol{d}} = \pi \boldsymbol{NA}^2 \tag{11}$$

and so the expected number of photons detected per second is

$$\langle n_0 \rangle = \frac{2\pi^2 \boldsymbol{NA}^4 \boldsymbol{P}}{\lambda hc} \frac{\partial \sigma}{\partial \Omega} \tag{12}$$

The sample volume is defined by the Gaussian beam shape. For a circular beam with numerical aperture NA and crossing angle ϕ, the beam waist is $w_0 = \lambda/(\pi NA)$, and (assuming $\phi \ll 1$ and ignoring a fixed phase factor $e^{i\phi}$), the ac photocurrent due to a particle at the centre of the beam is given by

$$\boldsymbol{i}_{ac} \approx 2\sqrt{\boldsymbol{i}_{LO} q Q n_0} \exp\left(\boldsymbol{i} 2\pi f_{\boldsymbol{d}} t - \left(\frac{2(x^2+y^2)}{w_0^2} + \frac{z^2 \boldsymbol{\phi}^2}{2w_0^2} \right) \right) \tag{13}$$

where Q is the quantum efficiency and f_d is the Doppler frequency.
The beam scans in the x direction at velocity v_x, so that for a particle at $(0,y,z)$, the complex detected photocurrent is

$$\boldsymbol{i}_{ac}(t) = 2\sqrt{\boldsymbol{i}_{LO} e Q n_0} \exp\left(\boldsymbol{i} 2\pi f_{\boldsymbol{d}} t - \left(\frac{2 v_x^2 t^2}{w_0^2} \right) \right) \exp\left(-\left(\frac{2y^2}{w_0^2} + \frac{z^2 \boldsymbol{\phi}^2}{2w_0^2} \right) \right)$$

In order to optimize the SNR, this signal must be filtered before detection. Since the signal is immersed in white noise, the rms noise increases as the square root of the filter bandwidth. For small bandwidths, the signal amplitude increases linearly, until most of the signal power is passing through the

filter, at which point the signal amplitude becomes nearly independent of the bandwidth. The optimal filter from a SNR point of view (ignoring the time spreading of the filtered signal) is one whose transfer function is the complex conjugate of the pulse spectrum; for a Gaussian pulse, the signal amplitude is reduced by a factor of $\sqrt{2}$. The length of the burst is increased by the same factor; the noise bandwidth of the filter is

$$B_{noise} = \frac{v_x}{\sqrt{\pi}\, w_0} \tag{15}$$

In this case, the ratio of the peak signal to the rms noise is

$$\frac{i_{peak}}{\langle i_n \rangle} = \sqrt{\frac{\sqrt{\pi}\, Q n_0 w_0}{v_x}} \exp\left(-\frac{2y^2}{w_0^2} - \frac{z^2 \phi^2}{2 w_0^2} \right) \tag{16}$$

The level curves of this function in the *yz* plane are ellipses. The volume scanned is the scan velocity times the cross-sectional area of the envelope in the *yz* plane. In order to achieve a false alarm rate of 1.2×10^{-5} Hz, as discussed above, we require a minimum value of $\alpha = I_{peak}(y,z)/\langle I_n \rangle$ of 7.12. Since the sensitivity varies continuously throughout the focal region, its envelope declining monotonically as we move away from centre, then if we want some finite sample volume, the central value must be somewhat higher than this. The area enclosed inside the contour $\{i_{peak}(y,z)/\langle i_n \rangle \geq \alpha\}$ is

$$A = \frac{\pi w_0^2}{2\phi} \ln\left(\frac{\sqrt{\pi} Q n_0 w_0}{\alpha^2 v_x} \right) \tag{17}$$

Because of the uncertainties due to additive noise and the random phase of the carrier of the tone burst, the thresholding operation is necessarily stochastic; however, a deterministic approximation provides a useful guide. If we assume that any signal whose peak value exceeds α times the rms noise is detected, the volumetric sampling rate R is equal to the area of the ellipse times v_x,

$$R = \frac{\pi w_0^2 v_x}{2\phi} \ln\left(\frac{\sqrt{\pi} Q n_0 w_0}{\alpha^2 v_x} \right) \tag{18}$$

This expression can be maximized with respect to v_x. The optimal value of v_x is

$$v_x\big|_{opt} = \frac{\sqrt{\pi} Q n_0 w_0}{\alpha^2 e} \tag{19}$$

resulting in a sampling rate of

$$R_{\max} = \frac{\sqrt{\pi} w_0^3 n_0 Q}{\alpha^2 e \phi} = \frac{2\lambda^2 Q N A P}{\sqrt{\pi}\, \alpha^2 e \phi h c} \frac{\partial \sigma}{\partial \Omega} \tag{20}$$

Since the crossing angle ϕ should scale as a multiple of *NA* in order that the two beams should be well enough separated to reject the wall reflection, the minimum differential scattering cross section is essentially independent of the numerical aperture, and that at a given value of $\partial\sigma/\partial\Omega$, a fixed number of photons is required per litre inspected. The factor of λ^2 is in the denominator because for a fixed NA, the sample volume goes as λ^3, but the number of photons per watt goes as λ^{-1}, leaving a factor of λ^2. For the system presented here, with α=7.12, ϕ=0.045, *NA*=0.008, *P*=100 mW, λ=830 nm, and v=30 cm^3/s , the minimum cross section is 10^{-12} cm^2/sr.

Do not be misled by the factor of λ^2 in the numerator of (20); apart from resonant effects for specific

particle sizes, $\partial\sigma/\partial\Omega$ decreases more rapidly than $1/\lambda^2$ everywhere, so better performance will be achieved at shorter wavelengths for constant beam power.

The sampling rate follows this dependence is verified qualitatively by the data of Figure 2, taken with particles well above the minimum size. Here the threshold was fixed, and the signal level varied with a switched attenuator in the amplified signal before filtering. The falloff in the sampling rate follows the prediction closely, as one would expect, since the noise is decreasing as the signal does, so that the stochastic character is less pronounced.

A more representative test is to reduce the signal level by changing the particle size instead, which led to the data of Figure 3. Here the agreement is merely qualitative, but the sharp cliff where the signal disappears below the threshold is clearly evident (the 0.008 NA system recorded 0 counts for 0.269 and 0.223 μm particles). The 0.48μm particles were on a steep slope of $\partial\sigma/\partial\omega$, so the low results recorded by both sensors probably reflect errors in wavelength, refractive index, or particle diameter.

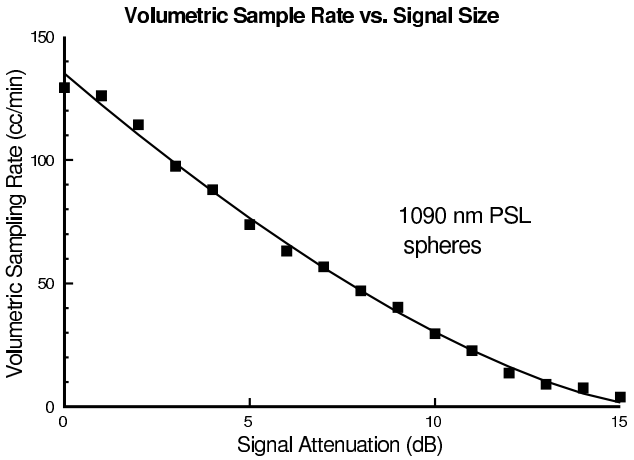

Figure 2: Volumetric sampling rate of the ISICL sensor on 1.09μm polystyrene latex spheres, as a function of signal attenuation.

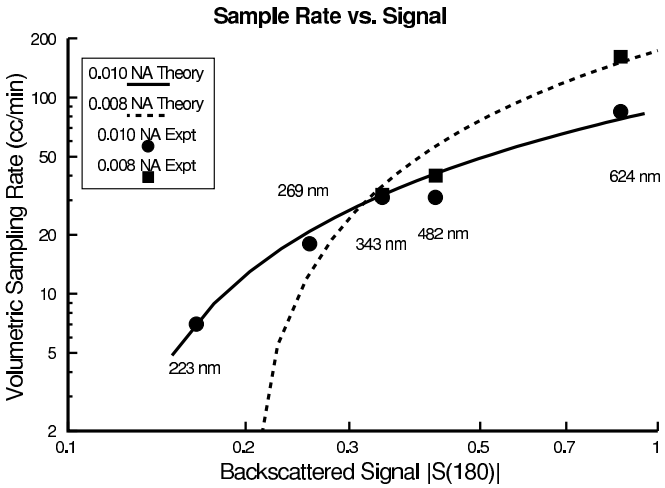

Figure 3: Volumetric sampling rate of the ISICL sensor vs. normalized differential scattering cross section (|S(180)| in Bohren's notation), using PSL spheres of different sizes.

3.3. Pulse Height Statistics

The pulse height digitizer used in ISICL uses a full wave successive-detection logarithmic detector, the signal level output of an FM radio IF amplifier IC. This detector is very inexpensive, and is logarithmic to within 1 dB or so over a 50 dB range. Since ISICL uses 8-bit digitizers and the pulse height information is coarse but has a wide dynamic range, this detection strategy is a good match.

The current output goes to a current-mode peak detector of conventional design. When a particle event occurs, the peak height is digitized after a suitable delay (10 μs or so), to make sure that the peak detector has captured the true peak of the tone burst. Otherwise, a large pulse would be digitized early on its rising edge, seriously understating the true peak value.

The logarithmically varying and somewhat poorly controlled bin widths make accurate predictions of the pulse height histogram difficult. Qualitatively, however, we expect that the histogram will have a steep falloff toward large pulses, since there is a unique maximum value when a particle crosses the beam axis, and only Gaussian noise broadens it. We expect more of a tail towards small pulses, though, because a small pulse may be due to a small particle going through the centre of the beam, or a large one crossing the wings. With a Gaussian transmit beam, this broadening should not be too great, since there is a faster than exponential falloff in the beam away from the axis. For particles near the lower sensitivity limit, the tail will be chopped

off since events far off axis will not break threshold.

The pulse height histograms shown in Figure 4 show this behaviour clearly. These plots were made with a variety of scan speeds, on both sides of the optimal speed. For reasonable departures from the ideal speed (0.2×-2×), the pulse height histogram shows only minor changes, allowing us to distinguish the 0.624 µm and 0.343µm spheres clearly.

4. EXPERIMENT

4.1. Test Apparatus Design

The test chamber used for these experiments was intentionally chosen to be smaller than optimum, 30 cm tall, 24 cm wide, and 15 cm deep. The working distance of the sensor is 30 cm. The beam entered the chamber via a side window made of fused silica and antireflection coated for 800nm, normal incidence. Monodisperse PSL aerosol was obtained with a PMS model PG-100 atomizer, which uses an ordinary medical atomizer used for inhaled drug delivery, with a small air pump, ultrafilter, and needle valves for atomizer and sheath gas feeds. The atomizer was loaded with NIST traceable PSL sphere suspensions from Duke Scientific and diluted with ultrapure water.

The chamber is attached to a PMS LAS-X aerosol spectrometer, which has excellent size resolution. We &fied that the particles were isolated by making sure that the particle size histogram did not change as the PSL sphere concentration was increased by a factor of 10, verifying that doublets are not present.

The possibility of dissolved solids in the water producing biased results was excluded by putting plain ultrapure water in the atomizer; a few counts at very small sizes (0.02 microns or so) are seen, corresponding to the residue in empty droplets. The shape of this background histogram changed only slightly when the Duke suspension was added, so any dissolved solids in the suspension are not a significant source of bias either.

In order to mimic worst-case, real world chamber walls, a sheet of bright sandblasted aluminum was used to line the back wall of the chamber. This material was found empirically to produce the worst mode hopping behaviour in the ISICL laser.

4.2. Window Imperfections

The sensor works at low numerical aperture (0.008), so we anticipated that it would be tolerant

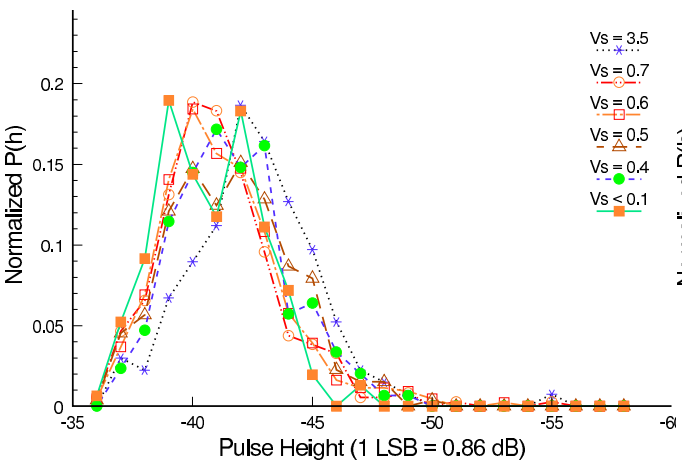

Figure 4a: ISICL pulse height histogram for PSL spheres of 0.343 µm +- 0.01 µm diameter, as a function of scan conditions. Only slight variations in the pulse height histogram are seen.

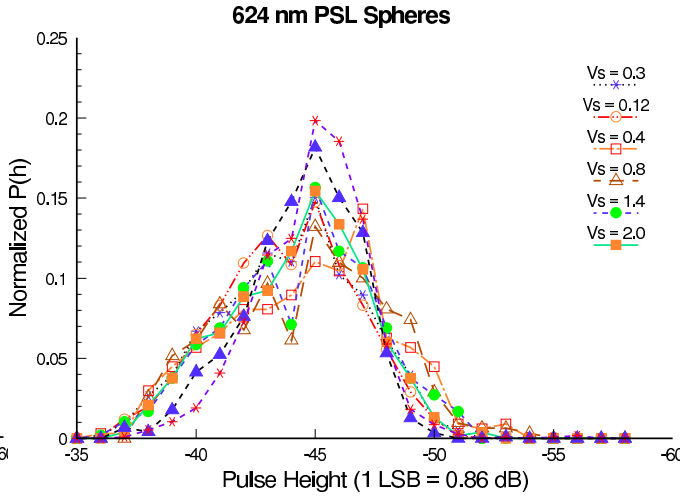

4b. Pulse height histogram for 0.624 µm PSL spheres at various scan speeds.

of imperfect windows. The scattered light returns through the window somewhat offset from the transmit beam; if there is severe waviness in the window, the sensitivity peak of the detector and transmit beam waist may fail to coincide, and in very bad cases, the two may miss one another altogether. We found that every O-ring sealed window we tried was satisfactory, while every glass-to-metal seal type window degraded the measurement sensitivity badly. The glass-to-metal seal windows are noticeably wavy, with a visually noticeable level of distortion of objects viewed through them.

Besides waviness, windows in plasma chambers often become etched or covered with films or dendrites. Any window which looks opaque will be a problem, but a moderate level of griminess is acceptable. To test this, we set up the sensor, shining the beam on a gold mirror (through a neutral density filter), and aligning the mirror carefully so that the reflected beam coincided with the local oscillator beam. We moved the mirror in and out with a translation stage, causing the phase of the reflected beam to vary rapidly, and measured the peak to peak variation in the differential optical signal, comparing it with its theoretical value, $4(i_{LO}i_{sig})^{1/2}$; the ratio of these two amplitudes gives the efficiency of the interference. In order to faithfully reflect actual operating conditions, no attempt was made to correct the polarization changes due to the presence of the windows. With no window, we achieved 95% efficiency; with a 0.5 inch thick fused quartz (not optical quality) window, it was 93%, independent of the angle of tilt of the window (up to 45 degrees in either plane), and it was still 75% with the quartz window smeared with greasy fingerprints and covered with a weathered piece of 1/4 inch acrylic sheet, although in that case, the received power was diminished by several decibels, which will reduce the sensitivity as well. The actual particle count data are not as sensitive as the interference efficiency measurement, but as a check, we put the 1/2 inch thick quartz window in front of the test chamber, tilted near normal and near 45 degrees, in pitch and in yaw; in all three cases, apart from the effect of Fresnel losses at the surfaces of the quartz, no change was evident in the data (less than a 5% sample volume reduction).

While ISICL works well with a variety of window configurations, it is less tolerant of windows made of birefringent materials such as sapphire. Sapphire is sometimes used for windows on etch chambers, for its superior chemical inertness. Unfortunately, the only transparent form of sapphire is a birefringent crystal, whose indices of refraction differ by 0.008; in a 5 mm thick vacuum window made of randomly oriented sapphire, the single-pass phase retardation will be on the order of 12 μm, corresponding to many waves. This will seriously reduce the polarization selectivity of the ISICL interferometer, which relies on polarization effects for the beam splitting and recombination. Sapphire windows will need to be replaced with fused quartz ones, coated with a thin layer of sapphire or other chemically inert, transparent material.

CONCLUSION

ISICL is a successful sensor for detecting and mapping submicron particles.
A simple deterministic model of signal detection in noise seems to explain the observed volumetric sampling rate vs. signal size dependence. The agreement is very good when the noise is reduced along with the signal, but less spectacular when the noise remains constant. Nonetheless, the qualitative features of the sampling rate vs. particle size performance are predicted correctly.

The falloff in sensitivity with distance from the centre of the beam intersection zone means that a given sized particle can give a tone burst of any size up to a maximum value depending on its backscatter differential scattering cross-section $\partial\sigma/\partial\Omega$. This leads to a tail toward small pulse heights, but the effect is not particularly strong owing to the faster than exponential falloff of the pulse height with distance. In an ensemble, the pulse height histograms do not depend strongly on scan speed, and so are a reasonable way to distinguish large particles from small.

The instrument appears to be very tolerant of poor window quality, including thick quartz plates at large angles to the beam, and smeared with grease. Within broad limits, even strong back-wall scattering of the laser beam does not degrade instrument behaviour, although the scattered light is 10^6 times stronger than the (50 photon) minimum detectable signal (in the detection NA). Even bright plasmas do not degrade the

measurement.

The good, predictable performance of the ISICL instrument, in the face of far from ideal chamber conditions, makes it a good instrument for sizing particles in confined and hostile spaces such as plasma chambers. We anticipate that this instrument will be commercially available soon, so that it can be used in real manufacturing situations.

REFERENCES

1. Philip C. D. Hobbs, "ISICL: in-situ coherent lidar for particle detection in semiconductor processing equipment", *Applied Optics* **9**, pp. 1579-90 (March 1995).

2. John R. Mitchell and Brian A. Knollenberg, "New techniques move in situ particle monitoring closer to the wafer, *Semiconductor International*, Sept. 1996 pp. 145-54

3. A. V. Jelalian, *Laser Radar Systems*, (Artech House, Boston, 1992) pp.33-41

4. Philip C. D. Hobbs, "Ultrasensitive laser measurements without tears", accepted for publication in *Applied Optics*, July 1996.